Available online at www.sciencedirect.com
SCIENCE DIRECT
Journal of Power Sources 140 (2005) 370–375
JOURNAL OF POWER SOURCES
www.elsevier.com/locate/jpowsour

Short communication

Local structure and redox energies of lithium phosphates with olivine- and Nasicon-like structures

A. Ait Salah[a], P. Jozwiak[b], J. Garbarczyk[b], K. Benkhouja[c], K. Zaghib[d,*], F. Gendron[a], C.M. Julien[a,*]

[a] LMDH, CNRS-UMR 7603, Université Pierre et Marie Curie, 140 rue de Lourmel, 75015 Paris, France
[b] Faculty of Physics, Warsaw University of Technology, Koszykowa, 7500-662 Warsaw, Poland
[c] LMCM, Université Chouaib Doukkali, BP20, El Jadida 24000, Morocco
[d] Institut de Recherches d'Hydro-Québec, 1800 Boul, Lionel-Boulet, Varennes, Québec, Canada J3X 1S1

Received 29 July 2004; accepted 28 August 2004
Available online 18 October 2004

Abstract

An experimental relationship between local structure and electrochemical properties is established for lithium metal phosphates $LiMePO_4$ (Me = Fe, Co, Mn), $LiFeP_2O_7$ and $Li_3Fe_2(PO_4)_3$ which crystallise with either the olivine-like or the Nasicon-like structure. Structural features of several lithium metal phosphates are investigated by a local probe such as the FTIR spectroscopy in order to explain the influence of either PO_4^{3-} or $P_2O_7^{4-}$ covalent bonds on redox energies. The local cationic arrangement is also discussed with the aid of a molecular vibration model to figure out the strong covalent bonds within a PO_4^{3-} complex for glassy Nasicon compounds.

Keywords: Lithium metal phosphates; Li-ion batteries; FTIR spectroscopy; Phospho-olivines; Diphosphates; Nasicon

1. Introduction

Among the well-known Li-insertion compounds used as positive electrodes in Li-ion batteries, the layered rock-salt systems $Li_{1-x}CoO_2$, the manganese-spinel framework system $Li_{1-x}Mn_2O_4$ and the phospho-olivine $LiFePO_4$ structures are now studied extensively [1–3]. Each of these materials has a specific capacity higher than 100 mAh g^{-1} combined with a discharge voltage between 3.4 and 4.8 V versus Li/Li^+. Another class of iron-containing oxides, namely $Li_3Fe_2(PO_4)_3$ with a Nasicon-like structure presents also interesting electrochemical properties [4,5].

The strongly condensed framework of lithium metal phosphates (LMPs) presents different physical and spectroscopic properties according the various polyanionic environments. Phospho-olivine structure is built from LiO_6 and FeO_6 octahedra linked to PO_4^{3-} polyanions whereas FeO_6 octahedra share no edges with other polyhedra in Nasicon-like structure. The internal electrostatic field changes when the structure does (from orthorhombic $LiFePO_4$ to monoclinic $Li_3Fe_2(PO_4)_3$, for instance), whereas the covalence of the Fe–O bond differs with the degree of covalence in the P–O bond. Electrochemical results show that the Fe^{3+}/Fe^{2+} level lies lower in the ordered olivine structure than in the Nasicon-like framework giving a higher voltage versus lithium [3].

In this work, we study the relationship between local structure and electrochemical properties of various LMP phases: $LiFePO_4$, $LiCoPO_4$, $LiMnPO_4$, $LiFeP_2O_7$, and $Li_3Fe_2(PO_4)_3$ which crystallise with either the olivine-like or the Nasicon-like structure. The local cationic arrangement is discussed with the aid of a molecular vibration model to figure out the strong covalent bonds within a PO_4^{3-} complex. We present here the results obtained from structural charac-

* Corresponding author. Tel.: +1 450 652 8019; fax: +1 450 652 8424.
E-mail addresses: karimz@ireq.ca, zaghib.karim@ireq.ca (K. Zaghib).

0378-7753/$ – see front matter © 2004 Elsevier B.V. All rights reserved.
doi:10.1016/j.jpowsour.2004.08.029

Table 1
Description of the lithium metal phosphates studied in this work

Compound	Synthesis	Structure	Space group	Lattice parameters
$LiFePO_4$	Wet chemistry using iron nitrate $Fe(NO_3)_3{\cdot}9H_2O$, and LiH_2PO_4 in distilled water	Orthorhombic olivine-like	*Pnma*	a = 5.917 Å; b = 10.209 Å; c = 4.698 Å
$LiCoPO_4$	Solid-state reaction using Li_2CO_3, $CoCO_3$, and $(NH_4)H_2PO_4$	Orthorhombic olivine-like	*Pnma*	a = 5.919 Å; b = 10.200 Å; c = 4.689 Å
$LiMnPO_4$	Solid-state reaction using Li_2CO_3, $MnCO_3$, and $(NH_4)H_2PO_4$	Orthorhombic olivine-like	*Pnma*	a = 6.102 Å; b = 10.445 Å; c = 4.742 Å
$LiFeP_2O_7$	Wet chemistry using LiH_2PO_4, $NH_4H_2PO_4$, and $Fe(NO_3)_3{\cdot}9H_2O$	Monoclinic pyrophosphate	$P2_1$	a = 4.821 Å; b = 8.083 Å; c = 6.939 Å; β = 109.38
$Li_3Fe_2(PO_4)_3$	sol–gel method using nitrate precursors	Orthorhombic Nasicon-like	*Pcan*	a = 8.827 Å; b = 12.3929 Å; c = 8.818 Å
$Li_3Fe_2(PO_4)_3$	Melt-quenching method using $LiNO_3$, Fe_2O_3, and $(NH_4)H_2PO_4$	Locally Nasicon-like	–	Glass
$Li_5V_2(PO_4)_5$	Melt-quenching method using $LiNO_3$, V_2O_5, and $(NH_4)H_2PO_4$	Locally Nasicon-like	–	Glass
$Li_3Mo_2(PO_4)_3$	Melt-quenching method using $LiNO_3$, MoO_3, and $(NH_4)H_2PO_4$	Locally Nasicon-like	–	Glass

terisation using a local probe such as the Fourier transform infrared (FTIR) spectroscopy in order to explain the influence of the PO_4^{3-} covalent bonds on redox energies of LMPs.

2. Experimental

Microcrystalline LMP compounds were synthesized by either solid-state reaction or a wet-chemical technique (see Table 1). $LiFeP_2O_7$ was prepared by a solution method using LiH_2PO_4, $Fe(NO_3)_3{\cdot}9H_2O$ and $NH_4H_2PO_4$ as precursor materials [6]. In this technique, the pH of the solution was controlled at 4.0. $Li_3Fe_2(PO_4)_3$ was synthesized by the sol–gel method using nitrate precursors. The solvent was evaporated at 120 °C in air. The solid dry residue was preheated at 400 °C for 4 h and final synthesis was at 700 °C for 12 h in Ar ambient. The glassy Nasicon-like structure samples of $Li_5V_2(PO_4)_5$, $Li_3Fe_2(PO_4)_3$ and $Li_3Mo(PO_4)_3$ were prepared by the melt-quenching method described below. Appropriate amounts of pre-dried $LiNO_3$ (Aldrich Chemical Company), $(NH_4)H_2PO_4$ (POCh – Polish Chemicals) and one of the following oxides, depending on composition: V_2O_5 (ABCR Karlsruhe), Fe_2O_3 (POCh – Polish Chemicals) or MoO_3 (Aldrich Chemical Company) were thoroughly mixed in a mortar. Alumina crucibles filled with the powders were placed in an electric furnace, first at 750 °C for 10 min, and then heated at 950 °C for 5 min in air. The molten mixture was rapidly poured out onto stainless-steel plate and immediately covered by the second stainless-steel plate. Resulting samples had an average thickness of 0.7 mm. XRD patterns confirmed the amorphous state of samples under study.

Powder XRD data were obtained using Cu Kα radiation with a Philips X'Pert diffractometer. Infrared absorption spectra were recorded using a Bruker IFS113 vacuum FTIR interferometer. Samples were ground to fine powders, mixed approximately 1:300 with ICs, and vacuum pressed into translucent disks. In the far-infrared region (400–100 cm^{-1}), the vacuum bench apparatus was equipped with a 3.5 μm-thick Mylar beam splitter, a globar source, and a DTGS/PE far-infrared detector.

The discharge–charge cycle for the electrode was made in lithium cells with non-aqueous electrolyte. Measurements were carried out using a Macpile potentiostat in the galvanostatic mode in the potential range 5.0–2.0 V at current density 7.23 mA g^{-1} (C/12 rate). The lithium anode was used as reference electrode by pressing the lithium foil on stainless steel disk. The electrolyte used was 1M $LiPF_6$ salt dissolved in 2:1 EC/DMC solution (Selectipur Merck, Germany).

3. Results and discussion

The crystal chemistry of microcrystalline materials was analyzed from XRD patterns (not shown here). The refined lattice parameters of the materials are seen in Table 1. Lithium orthophosphates $LiMePO_4$ (Me = Fe, Co, Ni) adopt an olivine-related structure, i.e. orthorhombic system with *Pnma* space group, which consists of a hexagonal closed-packing (hcp) of oxygen atoms with Li^+ and Me^{2+} cations located in half of the octahedral sites and P^{5+} cations in 1/8 of tetrahedral sites [7,8]. This structure may be described as chains (along the c-direction) of edge-sharing MeO_6 octahedra which are cross-linked by the PO_4 groups forming a three-dimensional (3D) network. Tunnels perpendicular to the [0 1 0] and [0 0 1] directions contain octahedrally coordinated Li^+ cations (along the b-axis), which are mobile in these cavities.

The diphosphate $LiFeP_2O_7$, in which the PO_4 tetrahedra are linked by bridging oxygen to give P_2O_7 groups, crystallizes in the monoclinic system ($P2_1$ space group). The P_2O_7 groups are connected to the FeO_6 octahedron by sharing two oxygen corners, each belonging to a PO_4 unit. This induces

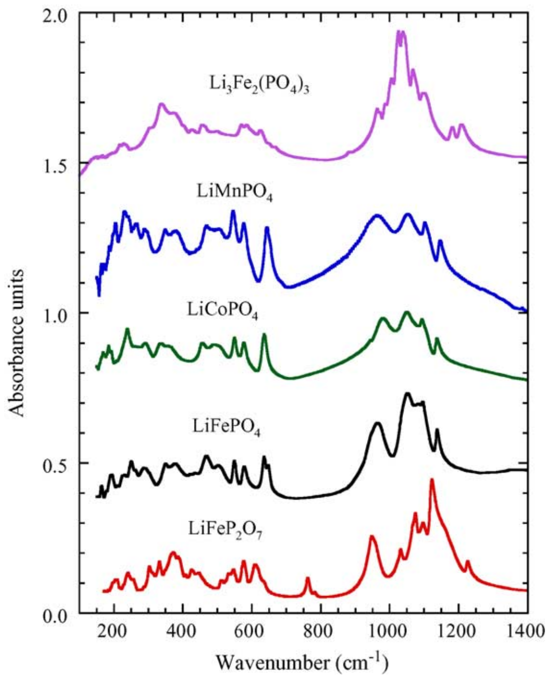

Fig. 1. FTIR absorption spectra of lithium metal phosphates with diphosphate ($LiFeP_2O_7$), olivine-like ($LiFePO_4$, $LiCoPO_4$, $LiMnPO_4$) and Nasicon-like $Li_3Fe(PO_4)_3$ framework.

a 3D framework in which channels collinear to the [0 0 1] direction are formed and where the lithium ions are located.

The Nasicon lattice may be described as a stacking of corner-sharing [$Me_2P_3O_{18}$] "lantern" units parallel to the *c*-direction. $Li_3Fe_2(PO_4)_3$ crystallizes in the orthorhombic system (*Pcan* space group). The lithium ions fully occupy three distinct crystallographic sites, two of which are in 5-fold co-ordination, Li(2) and Li(3), whereas Li(1) is in 4-fold coordination [9].

Fig. 1 shows the FTIR absorption spectra of LMPs with diphosphate $LiFeP_2O_7$, olivine-like $LiFePO_4$, $LiCoPO_4$, $LiMnPO_4$, and Nasicon-like $Li_3Fe(PO_4)_3$ framework. All these spectra are dominated by the internal vibrations (ν_1–ν_4) of the PO_4^{3-} units which involve the displacement of oxygen atoms of the tetrahedral PO_4^{3-} anions and present frequencies closely related to those of the free molecule. For $LiFePO_4$ phospho-olivine, these are a singlet (A_1) at a frequency $\nu_1 = 965\,cm^{-1}$; a doublet (E) at $\nu_2 = 465\,cm^{-1}$ and two triply degenerate (F_2) modes, ν_3 in the region 1050–1140 cm^{-1} and ν_4 in the range 500–560 cm^{-1}. ν_1 and ν_3 involve the symmetric and anti-symmetric stretching mode of the P–O bonds, whereas ν_2 and ν involve mainly O–P–O symmetric and anti-symmetric bending mode with a small contribution of P vibration [10,11]. In a solid, internal modes can split as a consequence of two effects: the site-symmetry effect due to an electric crystal field of symmetry lower than tetrahedral acting on the molecule and the correlation effect due to the presence of more than one molecular group in the crystal unit cell. In the far-IR region the external modes occur below 400 cm^{-1} where translatory and vibrational motions of the PO_4^{3-} ions and translatory motion of the Fe^{2+} ions are recorded. IR bands at 379 and 576 cm^{-1} show some FeO_6 contribution, while the band located at 251 cm^{-1} is attributed to the lithium-ion cage mode [12].

The FTIR spectrum of the $LiFeP_2O_7$ compound displays some differences with that of orthophosphates. Vibrational features of the diphosphate are as follows. (i) The low-wavenumber region is quite similar to that recorded for $LiFePO_4$. (ii) The IR stretching bands are shifted toward the high-wavenumber side due to the existence of $P_2O_7^{4-}$ units in C_2 site group. (iii) Additional IR bands appear at 763 and 954 cm^{-1} attributed to the anti-symmetric ν_{as} and symmetric ν_s stretching modes of P–O–P bridges. (iv) One high-wavenumber IR band is located at 1226 cm^{-1} assigned to the terminal stretching mode of $P_2O_7^{4-}$ ions. From the data shown in Fig. 1, it is obvious that diphosphate groups are bent in $LiFeP_2O_7$ structure as the symmetric and anti-symmetric bridge vibrations are active in infrared. The P–O–P bridge of $P_2O_7^{4-}$ group may be considered as an independently vibrating unit and within the limits of this approximation, its stretching frequencies depend on the value of the bridging θ angle, but also of the force constant of P–O bond of the bridge.

A large splitting of the ν_3 components of the PO_4^{3-} group is found for all phospho-olivine phases. This is due to the type of bonding between the oxygen and the Me octahedral cation which has necessarily an influence on the bonding between oxygen and the tetrahedral cation. In $LiMePO_4$ compounds, every oxygen is bonded to three octahedral cations, either two Fe^{2+} on sites of C_i symmetry and Li^+ on sites of C_1 symmetry. As a consequence, there is a correlation between the splitting ($\Delta\nu_3$) and the second ionization potential of the divalent cation as shown in Fig. 2. This result is in agreement with the origin of the splitting: a higher value of the second ionization potential of the octahedral cation Me^{II} implies a stronger interaction with the adjacent P–O bond. The most noticeable feature in vibrational patterns is the highest frequencies of

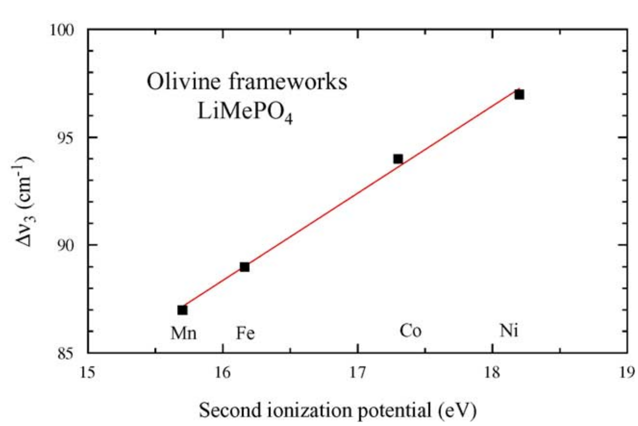

Fig. 2. Relation between the $\Delta\nu_3(PO_4)$ splitting and the second ionization potential in $LiMePO_4$ phospho-olivine compounds (Me = Mn, Fe, Co, and Ni).

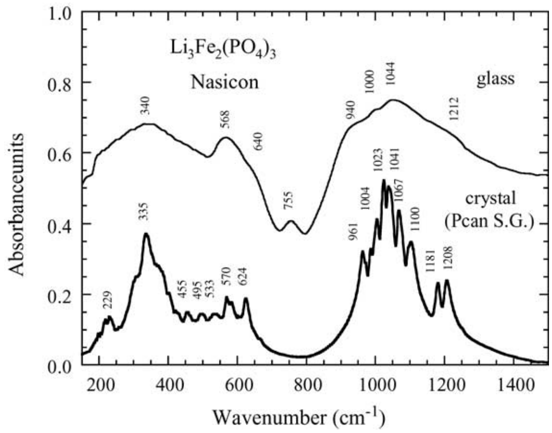

Fig. 3. FTIR absorption spectra of lithium iron phosphates with Nasicon-like framework for crystalline $Li_3Fe_2(PO_4)_3$ and vitreous $Li_3Fe_2(PO_4)_3$.

the ν_3 modes for the nickel phase. Also, the strong covalent bonds within the $(PO_4)^{3-}$ complex of $LiCoPO_4$ could explain the difference between redox energies.

Fig. 3 displays the FTIR absorption spectra of both crystalline and glassy $Li_3Fe_2(PO_4)_3$ Nasicon phases. The glass spectrum is approximately the envelope of the crystallized phosphate spectrum. As for other phosphates, internal modes involving the displacement of oxygen atoms of the pseudo-tetrahedral PO_4^{3-} anions of $Li_3Fe_2(PO_4)_3$ present frequencies closely related to those of the free molecule. The high-frequency band splitting with components observed at 1004, 1023, 1041, 1067 cm^{-1} in the IR spectrum is the manifestation of a correlation field effect due to the coupling of the PO_4 vibrators in the unit cell. Lantern units present in the Nasicon phases give rise to infrared bands in the range 1150–1250 cm^{-1} which are attributed to the stretching vibrations of terminal PO_3 units. These bands are located at 1181 and 1208 cm^{-1} for $Li_3Fe_2(PO_4)_3$. Both these two high-frequency spectral features and the strong band in the low-wavenumber region at 300–350 cm^{-1} are fingerprints for Nasicon-like structures. The FTIR spectrum of $Li_3Fe_2(PO_4)_3$ glass sample displays additional band centred at 755 cm^{-1} which is attributed to the P–O–P bonding occurring in the disordered Nasicon phase.

Fig. 4 shows the FTIR absorption spectra of glasses with $[Me_2(PO_4)]$ framework. Spectrum of $Li_5V_2(PO_4)_5$ glassy compound has the same features than the $Li_2O–V_2O_5–P_2O_5$ glass system. The high-frequency band around 1180 cm^{-1} due to P–O stretching along with the 750 cm^{-1} band due to P–O–P bending may be considered as evidence for the presence of $PO_4{}^{3-}$ pyrophosphate species in the glasses. Similar band was observed in Raman spectra of silver–phosphate glasses containing orthophosphate and pyrophosphate group [13] and in Raman spectra of silver–vanadate glasses containing metavanadate chains [14]. Although the spectra are dominated by vibrational features due to phosphate ions, transition-metal ions also register their presence in the middle region of 400–700 cm^{-1}.

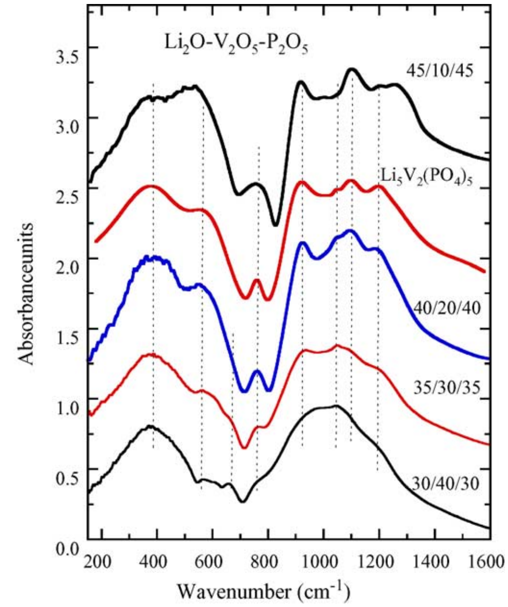

Fig. 4. FTIR absorption spectrum of vitreous $Li_5V_2(PO_4)_5$ with Nasicon-like random framework compared with spectra of selected glasses of the $Li_2O–V_2O_5–P_2O_5$ system. Numbers (e.g. 45/10/45) mean mol% of glass constituents.

Fig. 5a and b show the charge-discharge curve for the orthophosphates $LiMePO_4$ (Me = Fe, Co) with olivine-like framework. The typical two-phase redox reaction, i.e. $LiFePO_4 \rightleftarrows Li_{1-x}LiFePO_4 + xLi^+ + xe^-$, is observed by the presence of the plateau at 3.5 V versus Li/Li^+ for $LiFePO_4$ (Fig. 5a). Combined with discharge voltage between 3.4 and

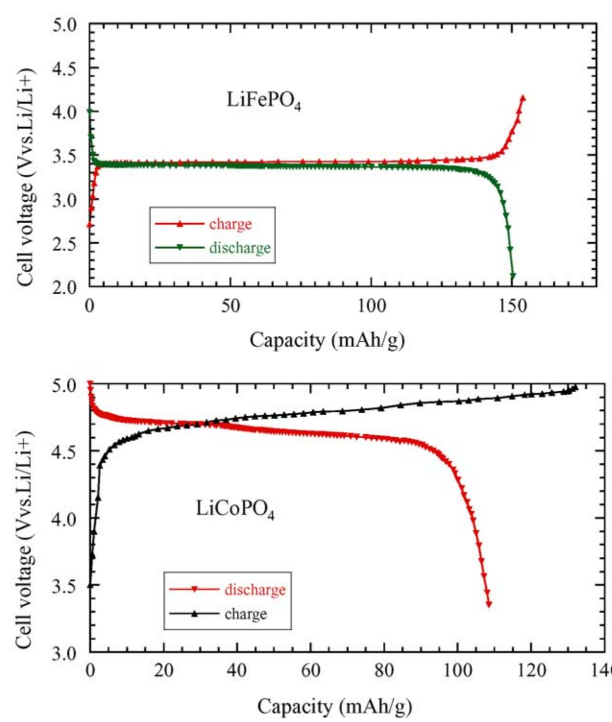

Fig. 5. Typical charge–discharge curves vs. Li/Li^+ for phospho-olivine frameworks (a) $LiFePO_4$ and (b) $LiCoPO_4$.

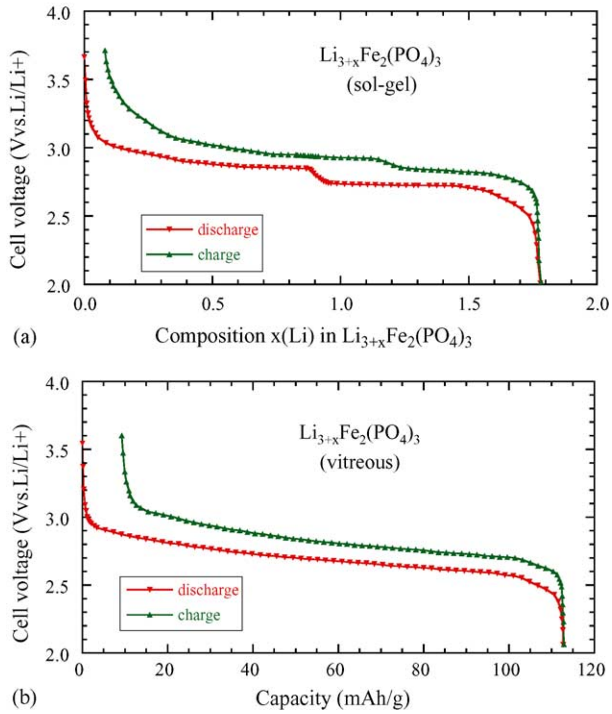

Fig. 6. Typical discharge–charge curves of $Li_3Fe_2(PO_4)_3$ vs. composition or capacity for (a) crystalline powder synthesized by sol–gel and (b) vitreous sample.

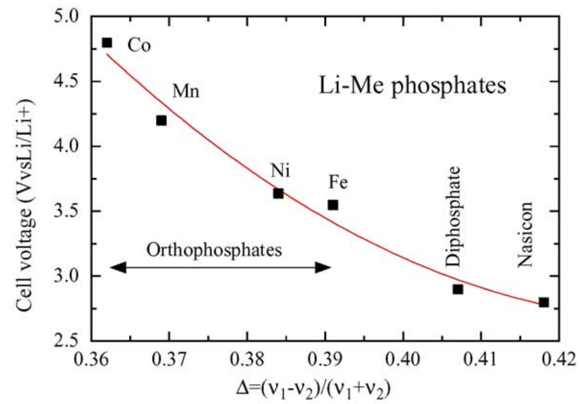

Fig. 7. Experimental relationship between covalency bonding factor obtained from FTIR data and cell voltage for lithium metal phosphates including: $LiCoPO_4$, $LiFePO_4$, $LiMnPO_4$, $LiFeP_2O_7$ and $Li_3Fe_2(PO_4)_3$.

4.8 V versus Li/Li^+, $LiFePO_4$ leads to high specific energy 150 mAh g^{-1}. These results are in good agreement with those reported in the pioneering work of Padhi et al. [2]. $LiCoPO_4$ shows a plateau at 4.72 V, extending up to 110 mAh g^{-1} in the discharge of the first cycle (Fig. 5b). The generation of an appropriately high voltage is due to the presence of the polyanion $(PO_4)^{3-}$ with strong Co–O covalency which stabilizes the antibonding Co^{2+}/Co^{3+} state through an Co–O–P inductive effect.

Fig. 6a and b show the typical discharge-charge curves of $Li_3Fe_2(PO_4)_3$: (a) crystalline powder synthesized by sol–gel and (b) vitreous sample. Complete lithium insertion leads to composition close to $Li_{4.8}Fe_2(PO_4)_3$ in which the transition metal cation is reduced to Fe^{2+}. The crystalline phase shows two well-defined plateaus at 2.85 and 2.70 V versus Li/Li^+ (Fig. 6a). These results are identical to those recently reported by Patoux et al. [15]. The existence of the intermediate phase $Li_4Fe_2(PO_4)_3$ is believed to be due to the lithium-ion insertion into crystallographic site generated by local reduction of the nearest iron positions. This is supported by a close examination of the FTIR spectrum of $Li_4Fe_2(PO_4)_3$ indicating a slight change of the stretching frequency of FeO_6 octahedra. From Fig. 6b, it is remarkable that the discharge–charge curves of vitreous $Li_3Fe_2(PO_4)_3$ occur without appearance of voltage plateau. This difference usually occurs between crystalline phase and glassy material in which distinct crystallographic sites are not well defined [16].

The energy of a given redox couple varies from one material to another depending on two main factors: (1) the electrostatic field at the cation position and (2) the covalent contribution to the cation–anion bonding. The study of both factors can be properly accomplished on oxides formed by MeO_6 octahedra (Me = transition metal cation) linked by tetrahedral polyanions $(PO_4)^{3-}$.

Investigations of framework structures built with polyphosphate anions have shown that the choice of the transition metal Me has a significant effect on the cell voltage as it is primarily dependent on the redox couple of the metal atom present in the structure [17]. The use of polyanions has shown the lowering Me^{3+}/Me^{2+} redox energy to useful levels in lithium cells. Polarization of the electrons of the O^{2-} ions into strong covalent bonding within the $PO_4{}^{3-}$ polyanion reduces the covalent bonding to the metal ion, which lowers its redox energy. The stronger the covalent bonding within the polyanion, the higher the voltage versus lithium displayed by the positive electrode.

Since vibrational spectra sensitive to the covalency of phosphate group, it is worthy to study a relationship between the relative energy levels and the covalency bonding in host structures having $PO_4{}^{3-}$ and $P_2O_7{}^{4-}$ anions. The useful estimate of a covalency strength is a parameter, Δ, defined by the relationship [18]

$$\Delta = \frac{\nu_1 - \nu_2}{\nu_1 + \nu_2} \tag{1}$$

where ν_1 and ν_2 are the internal mode wavenumbers of the phosphate anion.

Fig. 7 shows the empirical relationship between covalency bonding factor and cell voltage for several lithium metal phosphates including $LiCoPO_4$, $LiFePO_4$, $LiMnPO_4$, $LiFeP_2O_7$, and $Li_3Fe_2(PO_4)_3$. Among the compounds with olivine-like structure, the cell voltage versus Li/Li^+ are 3.55 V for $LiFePO_4$ and 4.75 V for $LiCoPO_4$. The cell voltage for LiMnPO4 has been reported to be 4.1 V versus lithium [19]. On the other hand, a cell voltage of 2.9 V is measured for the diphosphate $LiFeP_2O_7$ while 2.8 V for the Nasicon-like framework.

4. Conclusion

Structural properties of several phosphates resembling olivine, pyrophosphate, and Nasicon structure and composition have been examined using XRD and FTIR spectroscopy. The condensation effects seem to have only a limited influence on the general spectroscopic behaviour because the internal vibrations of the tetrahedral anions exhibit very similar frequencies as those found for the "free" PO_4^{3-} ions and the $P_2O_7^{4-}$ ions in solution.

Nevertheless, a comparison of the vibrational features shows that the spectral fingerprints can be unambiguously defined for lithium metal phosphates. For $LiMePO_4$ phospho-olivine structures, in the region of the internal modes of the phosphate anion, we identify the symmetric stretching mode at $\nu_1 = 965\,cm^{-1}$ and the triplets ν_3 in the regions $1000–1100\,cm^{-1}$. (Me = Ni, Co, Mn, Cu) possess a centrosymmetric structure. The dominant infrared spectral feature of diphosphate $LiFeP_2O_7$ is the appearance of the symmetric and anti-symmetric stretching vibration of P–O–P bridging bonds. The specific fingerprints of Nasicon-like framework are the infrared bands in the range $1150–1250\,cm^{-1}$ which are related to lantern units present in the $Li_3Fe_2(PO_4)_3$. An experimental relationship between spectral features of the local structure and electrochemical redox potential has been established for LMPs materials.

Acknowledgments

This work was partly supported by EU CEPHOMA project, contract No. ENK5-CT-2002-80666. A.A.S thanks the "Comité franco-marocain" for the financial support from (AI No. MA/03/71).

References

[1] A. Manthiram, J.B. Goodenough, J. Solid State Chem. 71 (1987) 349.
[2] A.K. Padhi, K.S. Nanjundaswamy, J.B. Goodenough, J. Electrochem. Soc. 144 (1997) 1188.
[3] S.-C. Yin, H. Grondey, P. Strobel, M. Anne, L.F. Nazar, J. Am. Chem. Soc. 125 (2003) 10402.
[4] C. Masquelier, A.K. Padhi, K.S. Nanjundaswamy, J.B. Goodenough, J. Solid State Chem. 135 (1998) 228.
[5] D. Morgan, G. Ceder, M.Y. Saidi, J. Barker, J. Swoyer, H. Huang, G. Adamson, Chem. Mater. 14 (2002) 4684.
[6] C. Wurm, et al., Chem. Mater. 14 (2002) 2701.
[7] S. Geller, J.L. Durand, Acta Crystallogr. 13 (1960) 325.
[8] I. Abrahams, J.L. Durand, Acta Crystallogr. 49 (1993) 925.
[9] A.B. Bykov, A.P. Chirkin, L.N. Demyanets, S.N. Doronin, E.A. Genkina, A.K. Ivanov-Shits, I.P. Kondratyuk, B.A. Maksimov, O.K. Melnikov, L.N. Muradyan, V.I. Simonov, V.A. Timofeeva, Solid State Ionics 38 (1990) 31.
[10] K. Nakamoto, Infrared and Raman Spectra of Inorganic and Coordination Compounds, Wiley, New York, 1978.
[11] M.T. Paques-Ledent, P. Tarte, Spectrochim. Acta 29A (1973) 1007.
[12] C.M. Burba, R. Frech, J. Electrochem. Soc. 151 (2004) 1032.
[13] R. Bacewicz, P. Woroniecki, J. Garbarczyk, Phys. Chem. Glasses 40 (1999) 124.
[14] R. Lewandowska, K. Krasowski, R. Bacewicz, J. Garbarczyk, Solid State Ionics 119 (1999) 229.
[15] S. Patoux, C. Wurm, M. Morcrette, G. Rousse, C. Masquelier, J. Power Sources 119–121 (2003) 278.
[16] C. Julien, Mater. Sci. Eng. R 40 (2003) 47.
[17] K.S. Nanjundaswamy, A.K. Padhi, J.B. Goodenough, S. Okada, H. Arai, J. Yamaki, Solid State Ionics 92 (1996) 1.
[18] A. Rulmont, R. Cahay, M. Liegeois, P. Tarte, Eur. J. Solid Inorg. Chem. 28 (1991) 207.
[19] G. Li, H. Azuma, M. Tohda, Electrochem. Solid-State Lett. 5 (2002) 135.